

Article

CHP-Based Economic Emission Dispatch of Microgrid Using Harris Hawks Optimization

Vimal Tiwari ¹, Hari Mohan Dubey ², Manjaree Pandit ¹ and Surender Reddy Salkuti ^{3,*}

¹ Department of Electrical Engineering, MITS, Gwalior 474005, India; vimaltiwari01@gmail.com (V.T.); manjaree_p@mitsgwalior.in (M.P.)

² Department of Electrical Engineering, BIT, Sindri 828123, India; hmdubey.ee@bitsindri.ac.in

³ Department of Railroad and Electrical Engineering, Woosong University, Daejeon 34606, Korea

* Correspondence: surender@wsu.ac.kr

Abstract: In this paper, the economically self-sufficient microgrid is planned to provide electric power and heat demand. The combined heat and power-based microgrid needs strategic placement of distributed generators concerning optimal size, location, and type. As fossil fuel cost and emission depend mainly on the types of distributed generator units used in the microgrid, economic emission dispatch is performed for an hour with a static load demand and multiple load demands over 24 h of a day. The TOPSIS ranking approach is used as a tool to obtain the best compromise solution. Harris Hawks Optimization (HHO) is used to solve the problem. For validation, the obtained results in terms of cost, emission, and heat are compared with the reported results by DE and PSO, which shows the superiority of HHO over them. The impact of renewable integration in terms of cost and emission is also investigated. With renewable energy integration, fuel cost is reduced by 18% and emission is reduced by 3.4% for analysis under static load demand, whereas for the multiple load demands over 24 h, fuel cost is reduced by 14.95% and emission is reduced by 5.58%.

Keywords: microgrid; combined heat and power; economic emission dispatch; renewable integration; TOPSIS



Citation: Tiwari, V.; Dubey, H.M.; Pandit, M.; Salkuti, S.R. CHP-Based Economic Emission Dispatch of Microgrid Using Harris Hawks Optimization. *Fluids* **2022**, *7*, 248. <https://doi.org/10.3390/fluids7070248>

Academic Editors: Ioannis K. Chatjigeorgiou, Dimitrios N. Konispoliatis and Mehrdad Massoudi

Received: 28 June 2022

Accepted: 13 July 2022

Published: 18 July 2022

Publisher's Note: MDPI stays neutral with regard to jurisdictional claims in published maps and institutional affiliations.



Copyright: © 2022 by the authors. Licensee MDPI, Basel, Switzerland. This article is an open access article distributed under the terms and conditions of the Creative Commons Attribution (CC BY) license (<https://creativecommons.org/licenses/by/4.0/>).

1. Introduction

In the past decades, the attention toward microgrid (MG) operation has increased with the integration of distributed generation (DG) units near the consumer end to fulfill the power demand. The MG has been characterized as a small-scale, self-sustaining cluster distribution power system architecture that combines multiple DG, combined heat and power (CHP) units, energy storage systems (ESSs), and load, acting as a single and controllable entity [1]. Integrating CHP units in the MG has attracted more attention with the motivation to provide thermal energy with electric power by using the waste heat generated during electricity generation [2]. The successful implementation of bio-inspired evolutionary optimization techniques in solving many complex engineering problems has attracted researchers to apply different optimization algorithms to solve the load dispatch problems using several test cases of power systems.

The combined heat and power dispatch (CHPED) problem has been realized using a real coded genetic algorithm [3], improved group search algorithm [4], oppositional teaching-learning based optimization [5], modified particle swarm optimization (PSO) [6], self-regulating PSO [7], cuckoo search algorithm (CSA) [8], gravitational search algorithm [9], exchange market algorithm [10], group search algorithm [11], and grey wolf optimization (GWO) [12] using different test cases. The demand-side management and the optimal operational problem of the MG were studied using a hybrid genetic algorithm (GA) and artificial bee colony (ABC) algorithm. Here, the objective is to minimize overall running costs of the MG, demand-side management costs, and costs due to load shifting [13]. A hybrid artificial neural network (ANN) and PSO model were used to

solve the biomass gasification plant (BGP) problem. This model was used to estimate the amount of biomass that was used to produce the required syngas, which is needed to meet the energy demand [14]. To enhance power exchange, the two-round fuzzy-based speed (TRFS) algorithm followed Stackelberg's game theory, and the Quasi-oppositional Symbiotic Organism Search Algorithm was used in a multi-MG environment to study the power exchange problem [15].

The power generating units using fossil fuels emit pollutant gases in the environment. These environmental concerns have pushed toward the integration of DGs based on clean and renewable resources. At the same time, emission constraints have also been considered in the scheduling problem. The economic dispatch and emission dispatch are single objectives to minimize the fuel cost and emission, respectively, by determining the optimal generation of each unit in the system while satisfying the demand load and other operational constraints. However, the results showed conflict with each other, i.e., minimizing fuel costs increases the emissions and vice-versa. Therefore, a multiobjective approach has been used to deal with these two conflicting objectives in the combined CHP economic and emission dispatch (CHPEED) problem. The CHPEED multi-objective problem has been solved using numerical polynomial homotopy continuation (NPHC) [16], the normal boundary intersection method [17], time-varying acceleration PSO [18], GWO [19], and multiverse optimization [20].

Integrating renewable-based DG such as wind and solar power with conventional units reduced environmental emissions. In Ref. [21], a comparative analysis was conducted to solve the power dispatch problem using different BI optimization methods for various test systems with the integration of wind units. The wind and fuel cell unit were integrated with the thermal plant to analyze economic dispatch and the MG power dispatch problem using CSA [22]. The solar and wind unit was incorporated with the thermal plant to investigate the CHPED using the squirrel search algorithm [23]. The impact on cost and emission with the integration of renewable-based DG was analyzed using an equilibrium optimizer (EO) [24]. The EED problem in a wind power integrated system was analyzed to estimate the impact of carbon trading prices on the reduction in carbon emission and enhancing the efficiency of power generation efficiency improvements [25]. To achieve the desired scenario of zero greenhouse gas emissions, the techno-economic feasibility analysis was carried out under different scenarios of the combined usage of renewable-based DG and storage systems [26]. The scheduling problem of MG having DG and wind units under their respective limits was performed using the manta ray foraging algorithm (MRFO). The effect on the cost due to the integration of solar power and energy storage systems was also examined [27]. The MG was reconfigured to analyze the demand response program using PSO to reduce the conventional DGs' fuel cost and the cost of acquiring electricity from the grid. The point estimate method was used to simulate the uncertainty of RESs, while the uncertainty due to other parameters was ignored [28]. A multiobjective thermal unit-based economic dispatch was carried out using binary and continuous PSO algorithms in Ref. [29]. To study the performance of MG under six distinct scenarios, the modified binary PSO was used to solve the load dispatch problem. The uncertainty of RESs, demand, and the market price was considered to neglect the system's power loss and spinning reserve [30]. The uncertainty associated with wind power plants due to uncertain wind velocity can be modeled using penalty and reserve cost to represent their under- and overestimation of wind power, respectively [31]. In Ref. [32], DE and PSO were used to analyze the planning problem in CHP-based MG. Here, the loss-sensitive approach was used to select the bus on a 14-bus MG and to determine the optimal size of DGs using PSO for minimum loss in the system, and CHPEED was further carried out using DE and PSO.

Wolpert and Macready, in the year 1997, proposed a No free lunch theorem, which states that no single algorithm can guarantee to solve all types of optimization problems [33]. Harris Hawks Optimization (HHO) is a swarm intelligence-based optimization approach; its analytical mode takes care of distinct foraging strategies such as tracing, sieging, and surprise attacks during the optimization process [34]. HHO has been successfully applied

for various real-world problems such as in cost management and the operation of multi-source-based microgrids [35], and in relay coordination problems [36]. In this paper, HHO was implemented for the solution of DG placement planning and optimum generation scheduling of a CHP-based MG.

The main contribution is as follows:

- The HHO algorithm was implemented to analyze its effectiveness in solving the DG placement and the load dispatch problem for an MG.
- Selection of optimal size and location of DGs for a 14-bus RDS.
- Load dispatch was conducted under two different scenarios (i.e., with and without renewable energy for minimization of cost and minimization of emission.
- TOPSIS was implemented to obtain the best-compromised solution (BCS).

This paper is organized as follows: Section 2 contains the problem formulation that combines the modeling of different types of DG units, the formulation of the CHPEED problem, and operational constraints. The concept behind the HHO algorithm is presented in Section 3. Section 4 deals with the description of test cases, simulation results, and discussion. Finally, concluding remarks are discussed in Section 5.

2. Problem Formulation

This paper focuses on CHPEED-based optimal generation scheduling for effective energy management planning in MG. Here, the objective is to minimize the cost and emission due to on-site generation and the CHP system. Therefore, optimal siting and sizing of DG units are essential in this context. Its formulations are added with the CHPEED problem as below.

2.1. Optimal Placement of DG

The DG unit was placed in MG to minimize the power loss as [32]:

$$\text{Minimum } (P_l) = \sum_{i=1}^{N_g} P_i - P_d \tag{1}$$

where P_l is the power loss in the system, P_d is the power demand, P_i is the power output of i^{th} DG unit, and N_g is the number of DG units in MG.

It is subject to the following constraints [32]:

$$V_{min} \leq |V_i| \leq V_{max} \tag{2}$$

where V_i is the voltage at the i^{th} bus, with minimum voltage $V_{min} = 0.95$ p.u. and maximum voltage $V_{max} = 1.05$ p.u.

$$P_i^{min} \leq P_i \leq P_i^{max} \tag{3}$$

where P_i^{min} and P_i^{max} are the minimum and maximum power output of the i^{th} DG unit, respectively.

2.2. Economic Dispatch

The total operational cost of all committed DGs units expressed as [22]

$$f_1 = F_{DG}^T + F_{WPP}^T + F_{FC}^T \tag{4}$$

where f_1 is the cost function; F_{DG}^T , F_{WPP}^T , and F_{FC}^T are the costs of conventional thermal generators, wind power plant (WPP), and fuel cell (FC) units over a period of time T , respectively [22,27].

2.2.1. Modeling of Conventional Thermal Generators

The fuel cost of conventional thermal generators is expressed as [32]

$$F_{DG}^T = \sum_{t=1}^T \sum_{i=1}^{N_g} \left(a_i \cdot (P_i^t)^2 + b_i \cdot P_i^t + c_i \right) \tag{5}$$

where a_i , b_i , and c_i are the fuel cost coefficient of the i^{th} DG unit. P_i^t is the power output of the i^{th} DG unit at the t^{th} interval of time and N_g is the number of DG units [32].

2.2.2. Modeling of Wind Power Plant

As the power generation of a wind power plant (WPP) is governed by uncertain wind velocity, its variable output characteristics are used to compute the cost of wind power. The cost of wind power generation includes the cost due to the uncertainty in it, expressed as [21,22,32].

$$F_{WPP}^T = \sum_{t=1}^T \sum_{j=1}^{N_w} C_j^t(P_{w_j}^t) \tag{6}$$

where N_w is the number of WPP units and

$$C_j^t(P_{w_j}^t) = \beta_{w_j} P_{w_j}^t + k_p (P_{w_j, av}^t - P_{w_j}^t) + k_r (P_{w_j}^t - P_{w_j, av}^t) \tag{7}$$

where $P_{w_j}^t$ and $P_{w_j, av}^t$ are the scheduled output and available wind power of the j^{th} unit at the t^{th} interval of time, respectively; β_{w_j} are the maintenance and operating cost in USD/kW; k_p and k_r are the penalty cost (underestimation) coefficient and reserve cost (overestimation) of the wind power plant, respectively [21,31]. These penalty costs and reserve costs of the wind power plant are, respectively, represented as [21,31]:

$$k_p (P_{w_j, av}^t - P_{w_j}^t) = k_p \int_{P_{w_j}^t}^{P_{w_r}} (P_w^t - P_{w_j}^t) f_w(P_w) dP_w \tag{8}$$

$$k_r (P_{w_j}^t - P_{w_j, av}^t) = k_r \int_0^{P_{w_j}^t} (P_{w_j}^t - P_w^t) f_w(P_w) dP_w \tag{9}$$

where P_{w_r} is the rated output of wind power and P_w^t is the output power of a wind power plant at the t^{th} time interval, determined as [21,31]:

$$P_w^t = \begin{cases} P_{w_r} \times \frac{(v^t - v_{cin})}{(v_r - v_{cin})} \text{ kW}, & ; \quad v_{cin} \leq v^t \leq v_r \\ P_{w_r} \text{ kW}, & ; \quad v_r \leq v^t \leq v_{co} \\ 0, & ; \quad v^t \leq v_{cin} \text{ and } v^t > v_{co} \end{cases} \tag{10}$$

where v^t is the wind velocity at the t^{th} time in m/s; v_{cin} , v_{co} , and v_r are the cut-in velocity, cut-out velocity, and rated velocity in m/s, respectively.

To determine the penalty and reserve costs, it is necessary to select the probability distribution function (*pdf*) for wind power output. The uncertainty and irregular nature of wind speed closely follow the Weibull distribution and *pdf* given as [21,31]:

$$pdf(v, k, c) = \frac{k}{c} \left(\frac{v}{c}\right)^{k-1} \exp\left(-\left(\frac{v}{c}\right)^k\right) \tag{11}$$

where k and c are *pdf* parameters referred to as the shape factor and scale factor, respectively. The corresponding cumulative distribution function (*cdf*) is given as [21,31]

$$cdf(v, k, c) = 1 - \exp\left(-\left(\frac{v}{c}\right)^k\right) \tag{12}$$

The probability of wind power is calculated as [21,31]

$$f_w(P_w) \left\{ P_w^t = P_{w_r} \times \frac{(v^t - v_{cin})}{(v_r - v_{cin})} \right\} = pdf(P_w) = \frac{klv_{cin}}{c} \left(\frac{(1+\rho l)v_{cin}}{c}\right)^{k-1} \exp\left(-\left(\frac{(1+\rho l)v_{cin}}{c}\right)^k\right) \tag{13}$$

where

$$\rho = \frac{P_w}{P_{w_r}}, \text{ and } l = \frac{(v_r - v_{cin})}{v_{cin}} \tag{14}$$

$$f_w(P_w)\{P_w^t = P_{w_r}\} = cdf(v_{co}) + (1 - cdf(v_r)) = \exp\left(-\left(\frac{v_r}{c}\right)^k\right) - \exp\left(-\left(\frac{v_{co}}{c}\right)^k\right) \quad (15)$$

$$f_w(P_w)\{P_w^t = 0\} = cdf(v_{cin}) + (1 - cdf(v_{co})) = 1 - \exp\left(-\left(\frac{v_{cin}}{c}\right)^k\right) + \exp\left(-\left(\frac{v_{co}}{c}\right)^k\right) \quad (16)$$

2.2.3. Modeling of Fuel-Cell Unit

The cost of an FC unit includes the cost of fuel and the efficiency of the fuel to generate electricity expressed as [22]:

$$F_{FC}^T = \sum_{t=1}^T \left(\beta_{natural} \sum_{i=1}^{N_{FC}} \frac{P_{FC,i}^t}{\eta_{FC,i}} \right) \quad (17)$$

where $\beta_{natural}$ is the operation and maintenance cost of FC in USD/kW; $\eta_{FC,i}$ and $P_{FC,i}^t$ are the efficiency and output power at the t^{th} time of the i^{th} FC unit, respectively [22].

2.3. Emission Dispatch

The emission released due to the burning of fossil fuel in the thermal power plants is expressed as follows [21,32]:

$$f_2 = \sum_{i=1}^{N_g} E_i^t(P_i^t) = \sum_{i=1}^{N_g} (\alpha_i \cdot (P_i^t)^2 + \beta_i \cdot P_i^t + \gamma_i) \quad (18)$$

where f_2 is total emission output; α_i , β_i , and γ_i are the emission cost coefficient of the i^{th} DG unit [31].

2.4. Formulation of Multiobjective CHPEED Problem

The multiobjective cost function of the CHPEED problem is given as [32]:

$$\text{minimize } (F) = w * f_1 + (1 - w) * f_2 * Pfn \quad (19)$$

where F is the total cost, Pfn is the price penalty factor, w is the weighting factor, and the Pfn is the ratio of fuel to the emission cost and is evaluated as:

$$Pfn_i = \frac{(a_i \cdot (P_i^{max})^2 + b_i \cdot P_i^{max} + c_i)}{(\alpha_i \cdot (P_i^{max})^2 + \beta_i \cdot P_i^{max} + \gamma_i)} \quad (20)$$

Equation (19) is minimized and subjected to operational constraints as follows [22,32].

2.5. Constraints

Total Power generation must be equal to sum of power demand and transmission loss. It is expressed as:

$$\sum_{i=1}^{N_g} P_i^t = P_d^t + P_l^t \quad (21)$$

where P_l^t is the power loss and P_d^t is the power demand at the t^{th} interval of time. P_l is evaluated as (22) [32]:

$$P_l^t = \sum_{i=1}^{N_g} \sum_{j=1}^{N_g} P_i^t \cdot B_{ij} \cdot P_j^t + \sum_{i=1}^{N_g} B_{0i} \cdot P_i^t + B_{00} \quad (22)$$

where B_{ij} , B_{0i} , and B_{00} are the loss coefficients.

Power generated by individual generator must vary within their minimum and maximum operating limit. It is expressed as:

$$P_i^{min} \leq P_i^t \leq P_i^{max} \quad (23)$$

$$P_{w,j}^{min} \leq P_{w,j}^t \leq P_{w,j}^{max} \quad (24)$$

$$P_{FC,i}^{min} \leq P_{FC,i}^t \leq P_{FC,i}^{max} \tag{25}$$

where $P_{FC,i}^{min}$ and $P_{w,j}^{min}$ are the minimum power output of FC and WPP units, respectively; $P_{w,j}^{max}$ and $P_{FC,i}^{max}$ are the maximum power output of WPP and FC units, respectively.

The change in power generating unit between two consecutive times is limited by up and down ramp limits, respectively, as follows [32]:

$$P_i^t - P_i^{t-1} \leq UR_i \tag{26}$$

$$P_i^{t-1} - P_i^t \leq DR_i \tag{27}$$

where UR_i and DR_i are up and down ramp limits of the i^{th} generating units, respectively [32].

$$H_R = \sum_{i=1}^{N_g} \theta_i \cdot P_i^t \tag{28}$$

where H_R is the total heat output and θ_i is the heat-to-power ratio of the i^{th} DG unit [32].

$$\sum_{i=1}^{N_g} \theta_i \cdot P_i^t \geq H_D \tag{29}$$

where H_D is the total heat demand.

2.6. TOPSIS

The technique of order preferences by the simulation to ideal solution (TOPSIS), initially proposed by Hwang and Yoon in 1981 [37], is a method to determine the optimal solution having the closest distance from the positive ideal solution and farthest distance from the negative ideal solution. The steps of the TOPSIS method are as follows:

Step I: Construct a decision matrix R as:

$$R = [x_{ij}], \quad i = 1, \dots, m; j = 1, \dots, n. \tag{30}$$

where x_{ij} is the value of the j^{th} attribute of the i^{th} alternative.

Step II: Normalize the decision matrix R as:

$$r_{ij} = \frac{x_{ij}}{\sqrt{\sum_{j=1}^m x_{ij}^2}}, \quad i = 1, \dots, m; j = 1, \dots, n. \tag{31}$$

Step III: Determine the weighted decision matrix as follows:

$$v_{ij} = w_j \times r_{ij}, \quad i = 1, \dots, m; j = 1, \dots, n. \tag{32}$$

Step IV: Determine the positive and negative ideal solution computed as follows:

$$A^+ = \{v_1^+, v_2^+, v_3^+, \dots, v_n^+\} \tag{33}$$

where

$$v_j^+ = \{(\max(v_{ij}), \text{if } j \in J_1) \text{ and } (\min(v_{ij}), \text{if } j \in J_2)\} \tag{34}$$

$$A^- = \{v_1^-, v_2^-, v_3^-, \dots, v_n^-\} \tag{35}$$

where

$$v_j^- = \{(\min(v_{ij}), \text{if } j \in J_1) \text{ and } (\max(v_{ij}), \text{if } j \in J_2)\} \tag{36}$$

Step V: Determine the separation distance of each alternative from positive and negative ideal solutions computed as follows:

$$D_i^+ = \sqrt{\sum_{j=1}^n (v_j^+ - v_{ij})^2}, \quad i = 1, \dots, m; j = 1, \dots, n \tag{37}$$

$$D_i^- = \sqrt{\sum_{j=1}^n (v_j^- - v_{ij})^2}, \quad i = 1, \dots, m; j = 1, \dots, n \quad (38)$$

Step VI: Compute the relative closeness (RC) of each alternative as:

$$RC_i = \frac{D_i^-}{D_i^- + D_i^+}, \quad i = 1, \dots, m; \quad (39)$$

An RC close to one indicates the superiority of the alternative.

3. Harris Hawks Optimization

Harris Hawks Optimization (HHO) is a population-based algorithm inspired by the foraging behavior of Harris Hawks, proposed by Heidari et al. in 2019 [34]. The analytical model of HHO simulates different foraging strategies such as tracing, sieging, and surprise attacks to capture prey during optimization. The cooperative foraging behavior of Harris Hawks is as follows:

- A prey for the Harris hawk is a rabbit having great escaping energy; therefore, several hawks cooperatively attack to prey simultaneously from different directions.
- This attack can be completed quickly, but sometimes considering the escape ability and behavior of the prey, it takes a few short-length, quick dives nearby the prey.
- The different phase of chasing a prey depends on the prey’s escaping pattern with other dynamic conditions.
- The switching strategy occurs when the best hawk (leader) stops and becomes lost on the hunt, and one of the other group members will pursue the chase.
- The Harris hawk can switch between these phases to confuse the prey, which leads to their exhaustion, and increases its vulnerability.
- Furthermore, by confusing the escaping prey, it cannot recover its defensive abilities and, in the end, it cannot escape from the team and encounter one of the hawks, which is often the most powerful and experienced, easily grabs the tired prey, and shares it with another group member.

Different phases of HHO are shown in Figure 1 [34].

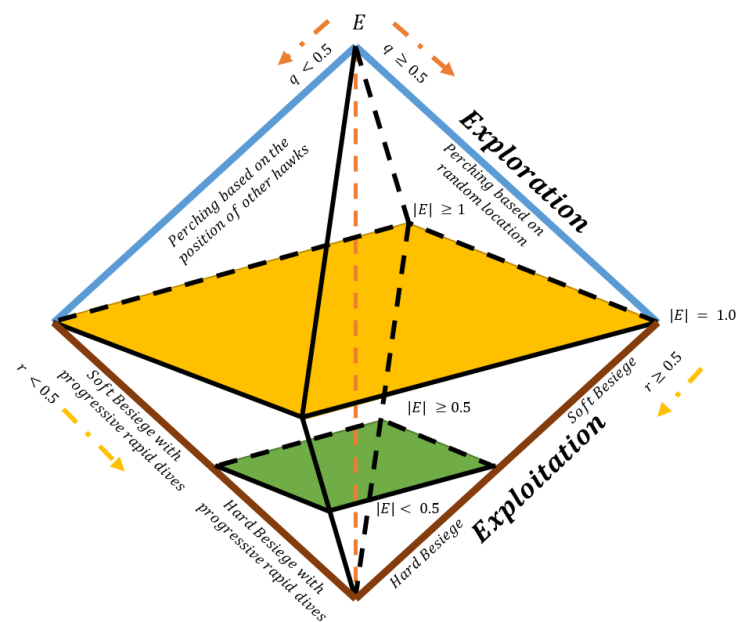


Figure 1. Different phases of HHO.

3.1. Exploration Stage

The hawks perch randomly to wait, observe, and monitor at some location to find prey based on two strategies. These strategies are mathematically modeled as:

$$X(t + 1) = \begin{cases} X_{rand}(t) - r_1 * |X_{rand}(t) - 2 * r_2 * X(t)|, & q \geq 0.5 \\ X_{rabbit}(t) - X_m(t) - r_3 * (LB + r_4(UB - LB)), & q < 0.5 \end{cases} \quad (40)$$

where $X(t + 1)$ is the position in the $(t + 1)^{th}$ iteration; X_{rabbit} is the position of the rabbit (prey); $q, r_1, r_2, r_3,$ and r_4 are random numbers in the interval $[0, 1]$. UB and LB are the upper and lower bounds, respectively. $X_m(t)$ is the mean position of the population evaluated as:

$$X_m = \frac{1}{N} \sum_{i=1}^N X_i(t) \quad (41)$$

where N is the population size, and $X_i(t)$ is the position of the i^{th} individual in the t^{th} iteration.

3.2. Transition from Exploration to Exploitation

In HHO, the rabbit's escaping energy ' E ' is used to transit between exploration and exploitation. The ' E ' decreases with an increase in the iterations and is evaluated as:

$$E = 2E_0 \left(1 - \frac{t}{T}\right) \quad (42)$$

where E_0 is the initial rabbit's escaping energy lying in the interval $[-1, 1]$; t and T represent the current and maximum number of iterations, respectively. As the iteration increases, E decreases from $[-2, 2]$ to 0. The exploration stage is used for $|E| \geq 1$, and for $|E| < 1$, the exploitation is carried out to search the prey.

3.3. Exploitation Stage

In the exploitation phase, four different strategies were adopted, and they were switched between by using escape energy ' E '; a random number r lies in the interval $[0, 1]$, representing successful prey escape. If $r < 0.5$, the prey escapes successfully, while $r > 0.5$ means the unsuccessful escape of the prey.

3.3.1. Soft Besiege

For soft besiege, $|E| \geq 0.5$ and $r \geq 0.5$ represent that the prey has enough energy to escape by jumping. Hence, hawks will hunt via a soft besiege strategy modeled as:

$$X(t + 1) = \Delta X(t) - E|J * X_{rabbit}(t) - X(t)| \quad (43)$$

where $\Delta X(t)$ represents the differences between the position of rabbits and current individuals, as given in (45). J represents the strength of the rabbit for randomly jumping during the escape and is evaluated with the random number r_5 as:

$$J = 2(1 - r_5) \quad (44)$$

$$\Delta X(t) = X_{rabbit}(t) - X(t) \quad (45)$$

3.3.2. Hard Besiege

For hard besiege, $|E| < 0.5$ and $r \geq 0.5$ represent that the prey's energy has exhausted, and hawks will hunt via a hard besiege strategy modeled as:

$$X(t + 1) = X_{rabbit}(t) - E|\Delta X(t)| \quad (46)$$

3.3.3. Soft Besiege with Progressive Rapid Dives

For soft besiege with progressive rapid dives, $|E| \geq 0.5$ and $r < 0.5$ represent that the prey has enough energy. Hence, hawks will hunt via soft besiege with the progressive rapid dives strategy modeled as:

$$Y = X_{rabbit}(t) - E|J * X_{rabbit}(t) - X(t)| \tag{47}$$

$$Z = Y + S \times LF(D) \tag{48}$$

where D is the dimension of the problem, S is a random vector of size $1 * D$, and LF is the levy distribution defined as

$$LF(x) = 0.01 \times \frac{\mu \times \sigma}{|\vartheta|^{1/\beta}}, \quad \sigma = \left(\frac{\Gamma(1 + \beta) \times \sin\left(\frac{\pi\beta}{2}\right)}{\Gamma\left(\frac{1+\beta}{2}\right) \times \beta \times 2^{\left(\frac{\beta-1}{2}\right)}} \right)^{1/\beta} \tag{49}$$

where μ and ϑ are random values that are between 0 and 1. β is the constant equal to 1.5.

The whole process at this stage is a mathematical model as:

$$X(t + 1) = \begin{cases} Y & \text{if } F(Y) < F(X(t)) \\ Z & \text{if } F(Z) < F(X(t)) \end{cases} \tag{50}$$

3.3.4. Hard Besiege with Progressive Rapid Dives

For hard besiege with progressive rapid dives, $|E| < 0.5$ and $r < 0.5$ represent that the prey loses its energy and becomes exhausted, and hawks will hunt via hard besiege with the progressive rapid dives strategy modeled as:

$$X(t + 1) = \begin{cases} Y & \text{if } F(Y) < F(X(t)) \\ Z & \text{if } F(Z) < F(X(t)) \end{cases} \tag{51}$$

where

$$Y = X_{rabbit}(t) - E|J * X_{rabbit}(t) - X(t)| \tag{52}$$

$$Z = Y + S \times LF(D) \tag{53}$$

The flow chart of HHO is shown in Figure 2.

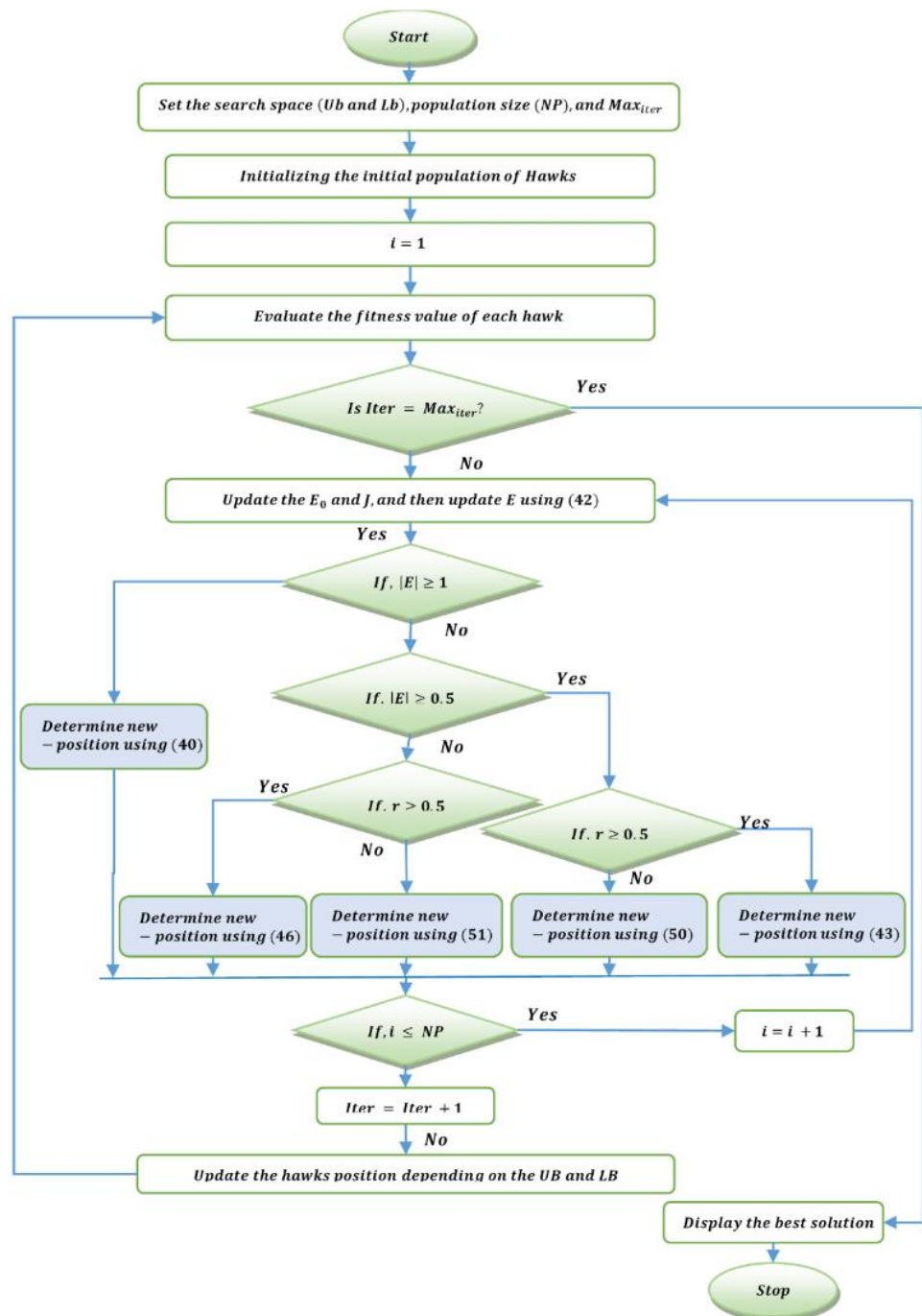


Figure 2. Flowchart of HHO algorithm.

4. Simulation Results

4.1. Description of Test Cases

The HHO algorithm was applied to find out the optimal size, its location of DG, and then the solution of the CHPEED problem in MATLAB R2016a, and it was executed on a CPU with an i5 processor and 4 GB RAM with a speed of 2.50 GHz. The parameter of HHO was considered, as the population size was 100 with a maximum iteration of 1000.

For this analysis, a hypothetical MG of a 14-bus RDS having 14 buses and 13 branches was considered, as shown in Figure 3. The line and load data are shown in Table 1 [32]. The utility providing the spinning reserve is represented as a virtual generator and connected to slack bus 1.

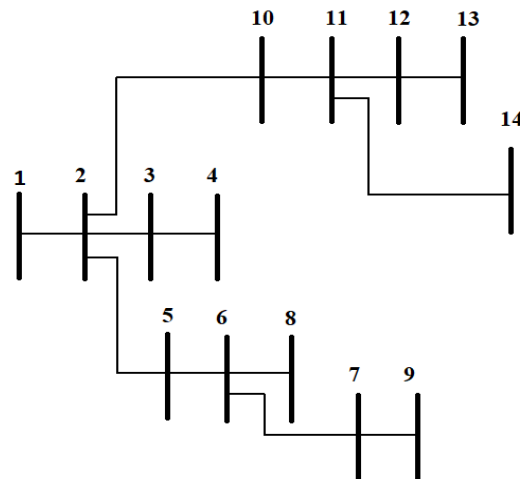


Figure 3. Single line diagram of 14-bus RDS.

Table 1. Line and load data of 14-bus RDS.

Bus No.	Start Bus	End Bus	R	X	Real	Reactive
1	0	0	0	0	0	0
2	1	2	0.0133	0.042	20	6
3	2	3	0.0194	0.059	85	27
4	3	4	0.0312	0.16	40	1
5	2	5	0.023	0.12	20	6
6	5	6	0.023	0.12	20	6
7	6	7	0.0193	0.059	76	16
8	6	8	0.032	0.084	10	30
9	7	9	0.034	0.17	61	16
10	2	10	0.016	0.042	12	75
11	10	11	0.193	0.059	10	90
12	11	12	0.067	0.17	16	61
13	12	13	0.04	0.1	90	59
14	11	14	0.05	0.15	35	61

The total static load demand was considered as (495 + j454) kVA. The initial real power loss without placement of DG units in RDS was 0.1995 kW with a minimum voltage of 0.9992 p.u. The simulation results for the placement of 4 DG units are given in Table 2. The optimal size of the 4 DGs with their best-suited location was obtained as 90.3178 kW (at bus 3), 187.9 kW (at bus 7), 114.9414 kW (at bus 13), and 44.8314 kW (at bus 14). The system power loss was reduced by 34.99% with a minimum voltage of 0.9995 p.u.

Table 2. Simulation results for 14-bus RDS.

Parameters	Without DGs	With 4 DGs
Power Loss (kW)	0.1995	0.1297
Loss Reduction (%)	-	34.99
DGs Size (kW) /Location	-	90.3178/3, 187.9/7, 114.9414/13, 44.8314/14
Total DG Size (kW)	-	437.9906
V_{min} (pu)	0.9992	0.9995
V_{max} (pu)	0.9998	0.9999

Analysis of the CHPEED was carried out for static load demand (SCHPEED) and for the multiple loads (MCHPEED) over 24 hr of a day with the following assumptions:

- (i) A two-diesel generator (Dg) with the sizes of 200 kW and 100 kW was selected and placed on buses 7 and 13, respectively. Similarly, the two microturbines (MTs) were

selected with the sizes of 80 kW and 30 kW and placed on buses 3 and 14, respectively. A Dg with the size of 500 kW was selected as a virtual generator to cover the peak demand of 495 kW.

- (ii) To analyze the impact of renewable energy integration(REI), the Dg of capacity 100 kW at bus 13 was replaced by a fuel cell (FC), the MT of 30 kW of bus 14 was replaced by a wind turbine with a capacity of 40 kW, and rest was the same as above.

The parameters of the wind turbine were considered as follows [31]:

Cut-in speed $v_{cin} = 5$ m/s; cut-out speed $v_{co} = 15$ m/s; rated speed $v_r = 45$ m/s. Weibull shape factor $k = 1.5$; scale factor $c = 5$; penalty cost coefficient $k_p = 5$; reserve cost coefficient $k_r = 5$.

The operational limits, fuel cost coefficient, emission coefficient, and heat rate data are listed in Table 3 [22,32]. For the planning of MG, the utility generator should be kept separately for participation in tracking the electric demand, i.e., at zero slack bus injection.

Table 3. Operational limits, fuel cost coefficient, emission coefficient, and heat rate data.

Type	Size (kW)	P_i^{min} (kW)	P_i^{max} (kW)	a_i	b_i	c_i	α_i	β_i	γ_i	Heat Rate (kJ/kWh)
Dg	500	0.00	500	10.193	105.18	62.56	26.55	-16.1836	7.0508	10,314
Dg	200	40	200	2.035	60.28	44.0	14.4296	-64.1535	130.4094	11,041
MT	80	16	80	0.5768	57.783	-133.0915	3.0358	-57.3403	311.5728	11,373
Dg	100	20	100	1.1825	65.34	44.0	19.38	-176.6946	821.6573	10,581
MT	30	6.0	30	0.338	89.1476	-547.619	1.0346	-60.384	943.1898	12,186
FC	100	0	100	0	0.07	0	0	0	0	0
WPP	40	0	40	0	0.22	0	0	0	0	0

The B-loss coefficients are as follows [32]:

$$B1 = 0.001 * \begin{bmatrix} 0.4355 & -0.1694 & 0.1482 & -0.2684 & -0.0925 \\ -0.1694 & 0.2366 & -0.0247 & -0.0061 & -0.0689 \\ 0.1482 & -0.0247 & 0.1636 & -0.2391 & -0.1046 \\ -0.2684 & -0.0061 & -0.2391 & 0.6517 & 0.1987 \\ -0.0925 & -0.0689 & -0.1046 & 0.1987 & 0.1864 \end{bmatrix}$$

$$B2 = 0.1 * [-0.0326 \quad -0.0314 \quad 0.0057 \quad -0.0018 \quad 0.0050]$$

$$B3 = [0.0014];$$

4.2. Discussion

4.2.1. Best Cost Solution

For the SCHPEED problem, as in Table 4, the best cost solution of HHO35.8483 USD/h is found to be better as compared to the reported result by DE [32]: 35.8974 USD/h and PSO [32]: 35.897USD/h. Table 5 shows that for SCHPEED with REI, the operational cost is found to be 29.3180 USD/h, which is lower as compared to SCHPEED by 18%, and all operational constraints (21), (23)–(25) are also satisfied.

Table 4. Generation schedule and comparative results for SCHPEED with demands of 338 kW.

Scenarios	Methods	P_1 (Dg)	P_2 (Dg)	P_3 (MT)	P_4 (Dg)	P_5 (MT)	Fuel Cost (USD/h)	Emission (g/kWh)	Heat (kWh)	Loss (kW)
Best Cost	HHO	0.00	157.09	80.00	73.1552	30.00	35.8483	45.4856	347.5639	2.2452
	DE [32]	0.00	166.30	80.00	64.30	30.00	35.8974	45.8467	348.048	—
	PSO [32]	0.00	166.68	80.00	63.89	30.00	35.897	45.870	348.000	—
Best Emission	HHO	0.00	168.8009	57.1848	96.0540	21.0526	36.9396	44.8121	329.3694	5.0922
	DE [32]	0.00	166.50	58.30	96.10	21.50	36.851	44.820	329.790	—
	PSO [32]	0.00	166.20	58.64	96.07	21.66	36.840	44.820	330.070	—
BCS	HHO	0.00	146.4312	80.00	89.92	24.7656	35.9695	45.0773	344.0685	3.1168
	DE [32]	0.00	150.54	80.00	90.92	20.55	36.0720	45.020	341.7225	—
	PSO [32]	0.00	150.20	80.00	89.86	21.95	36.0600	45.030	342.7200	—

BCS: Best Compromise Solution.

Table 5. Generation schedule and comparative results for SCHPEED with REI with demands of 338 kW.

Scenario	P_1 (Dg)	P_2 (Dg)	P_3 (FC)	P_4 (Dg)	P_5 (WPP)	Total Cost (USD/h)	Fuel Cost (USD/h)	Wind Cost (USD/h)	Emission (g/kWh)	Heat (kWh)	Loss (kW)
Best Cost	0.00	174.8425	95.6318	33.2694	39.8741	29.3180	27.5252	1.7928	48.1604	171.1845	5.6179
Best Emission	0.00	200.00	50.1720	100.00	0.4670	34.4114	34.2040	0.2074	43.2924	244.9725	12.6390
BCS	0.00	155.0687	92.0436	88.6900	9.1448	30.3835	29.9638	0.4197	44.3393	198.7907	6.9470

For the MCHPEED problem, the best cost solution is found to be USD 1203.0999, while USD 1023.3403 is for MCHPEED with REI as in Table 6. Their generation schedules are presented in Figures 4 and 5, respectively.

Table 6. Comparative results for MCHPEED and MCHPEED with REI.

Scenario	MCHPEED				MCHPEED with REI					
	Total Cost (USD)	Emission (g/kW)	Heat (kW)	Loss (kW)	Total Cost (USD)	Fuel Cost (USD)	Wind Cost (USD)	Emission (g/kW)	Heat (kW)	Loss (kW)
Min.Cost	1203.0999	1089.9256	15,587.8723	203.5641	1023.3403	1003.2465	20.0938	1085.8532	15,528.2799	167.1917
Min. Emis	1250.0066	1068.1567	15,918.5405	309.1087	1384.1995	1361.902	22.2975	1008.5490	17,674.5642	555.1573
BCS	1211.5507	1077.6050	15,588.9110	212.6814	1094.9539	1070.9602	23.9937	1050.8518	15,579.2478	253.8731

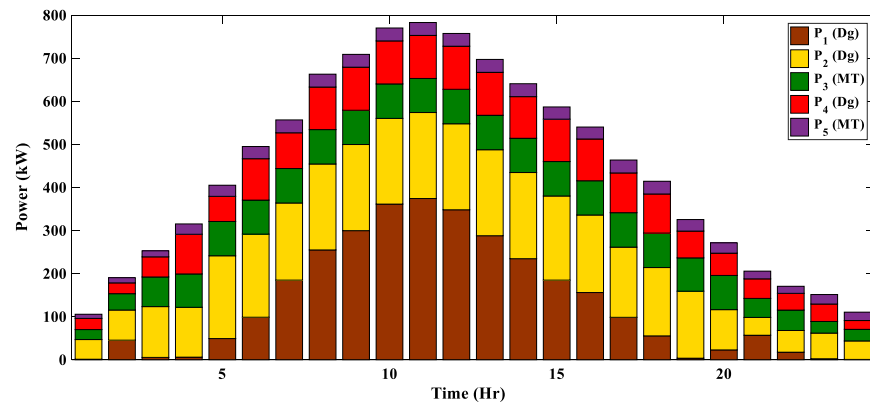


Figure 4. The generation scheduling of MSCHPEED for cost minimization.

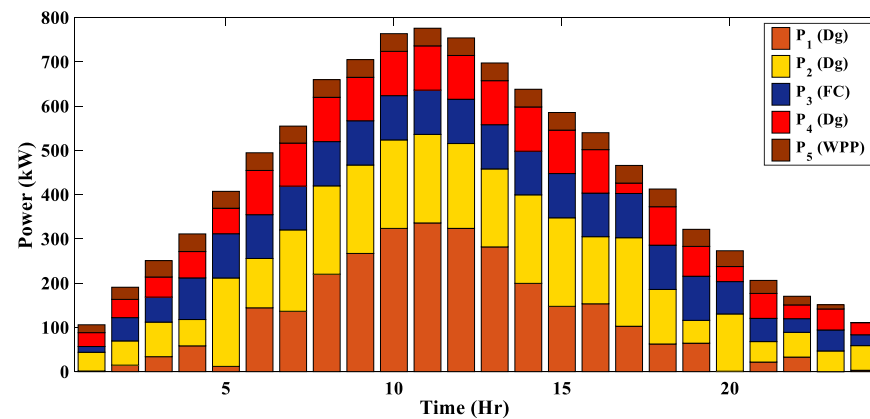


Figure 5. The generation scheduling of MSCHPEED with REI for cost minimization.

4.2.2. Best Emission Solution

The best emission solution, 44.8121 g/kWh, was obtained by HHO as in Table 4. It was found to be lower than 44.820 g/kWh reported using DE [32] and 44.820 g/kWh by PSO [32], which was further reduced to 43.2924 g/kWh for SCHPEED with REI as in Table 5.

For the MCHPEED problem, the best emission solution was found to be 1068.1567 g/kW and 5.58% lower than 1008.5490 g/kW for MCHPEED with REI as in Table 6. Figures 6 and 7 represent the generation schedule corresponding to the best emission solution.

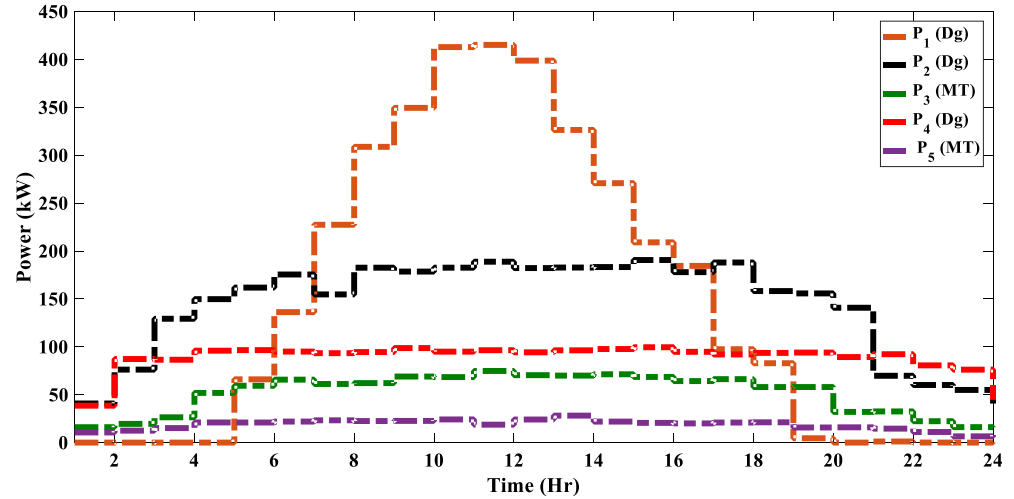


Figure 6. The generation scheduling of MSCHPEED for emission minimization.

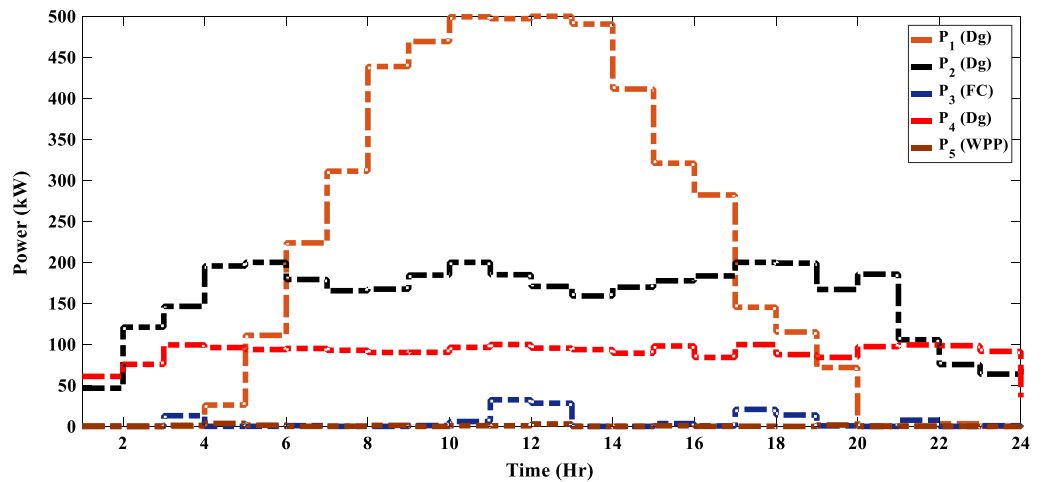


Figure 7. The generation scheduling of MSCHPEED with REI for emission minimization.

4.2.3. Best Compromise Solution

PPF is the weighted sum method to convert a multiobjective function into a single objective function. TOPSIS is used as a tool to rank the solution on the basis of the distance between positive and negative distance from the ideal solution. Tables 7 and 8 show the top ten optimal front solutions for SCHPEED and MCHPEED problems. The elite solution was selected on the basis of top rank, and the corresponding Pareto fronts are shown in Figure 8, and Figure 9, respectively. Table 4 shows that for SCHPEED, the BCS in terms of the fuel cost of 35.9695 USD/h and the emission of 45.0773 g/kWh was also found to be superior to the reported results by DE [32] and PSO [32]. Considering Table 5, the BCS of 30.3835 USD/h and 44.3393 g/kWh was found to be lower due to REI with a topsis rank of 0.7886 as in Table 7.

Table 7. Top ten Pareto optimal solution for SCHPEED.

S. No.	SCHPEED					SCHPEED with REI				
	Fuel Cost (USD/h)	Emission (g/kWh)	Mu_1	Mu_2	TOPSIS	Total Cost (USD/h)	Emission (g/kWh)	Mu_1	Mu_2	TOPSIS
1	35.9695	45.0773	0.002	0.0079	0.796	30.3835	44.3393	0.0111	0.0415	0.7886
2	36.0148	45.0389	0.002	0.0077	0.7941	30.5396	44.2242	0.0117	0.041	0.7784
3	35.8766	45.1944	0.0026	0.0083	0.7613	30.0147	45.1952	0.014	0.0407	0.7433
4	36.1974	44.96	0.0028	0.0067	0.7039	30.2459	45.2667	0.0153	0.0388	0.7172
5	35.8483	45.4856	0.0046	0.0083	0.6436	30.3843	45.336	0.0163	0.0376	0.698
6	36.4597	44.8753	0.0046	0.0056	0.5464	31.5101	43.9487	0.0182	0.0368	0.6697
7	36.6261	44.8394	0.0059	0.0051	0.4633	31.4086	44.444	0.0185	0.0349	0.6531
8	36.7405	44.8232	0.0068	0.0048	0.4177	31.8543	44.1804	0.0213	0.0339	0.6146
9	36.8258	44.8157	0.0074	0.0047	0.3901	29.6449	47.2935	0.0272	0.0388	0.5877
10	36.9396	44.8121	0.0083	0.0047	0.3614	29.318	48.1604	0.0329	0.041	0.5542

Table 8. Top ten optimal front solutions.

S. No.	MCHPEED					MCHPEED with REI				
	Fuel Cost (USD)	Emission (g/kW)	Mu_1	Mu_2	TOPSIS	Total Cost (USD)	Emission (g/kW)	Mu_1	Mu_2	TOPSIS
1	1211.551	1077.605	0.0342	0.1084	0.7602	1094.954	1050.852	0.1551	0.5313	0.7741
2	1216.566	1072.838	0.0381	0.1015	0.7268	1137.664	1039.921	0.2188	0.4576	0.6765
3	1216.921	1074.578	0.0406	0.0988	0.709	1175.755	1033.977	0.2841	0.3924	0.58
4	1203.1	1089.926	0.0561	0.1241	0.6888	1199.708	1030.557	0.3263	0.3522	0.5191
5	1221.714	1073.912	0.0509	0.0891	0.6365	1228.073	1028.583	0.3772	0.3045	0.4467
6	1222.0187	1082.3297	0.044	0.0578	0.5677	1260.982	1023.543	0.4362	0.2537	0.3677
7	1223.182	1087.8793	0.0522	0.0542	0.5093	1280.761	1022.409	0.4721	0.2236	0.3214
8	1227.4204	1086.4162	0.056	0.0471	0.4568	1306.819	1015.037	0.519	0.1947	0.2728
9	1230.0698	1089.8465	0.0635	0.0421	0.3983	1347.69	1013.701	0.5934	0.1521	0.204
10	1250.007	1068.157	0.1173	0.057	0.3272	1384.2	1008.549	0.6598	0.1465	0.183

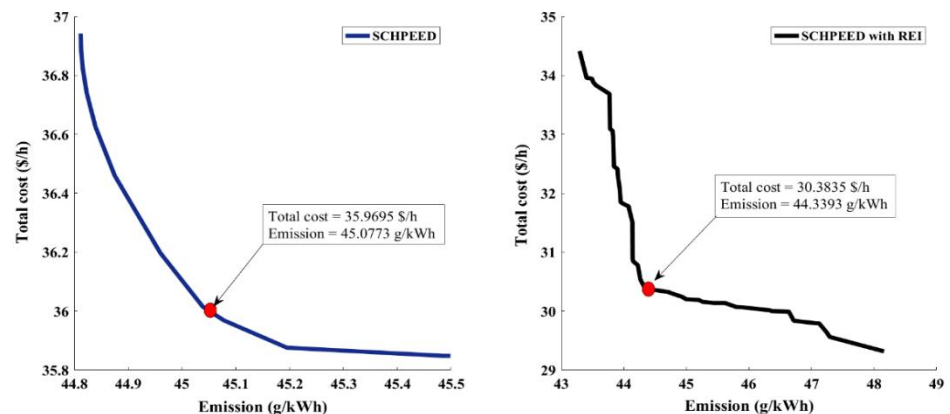


Figure 8. Pareto optimal fronts for SCHPEED and SCHPEED with REI.

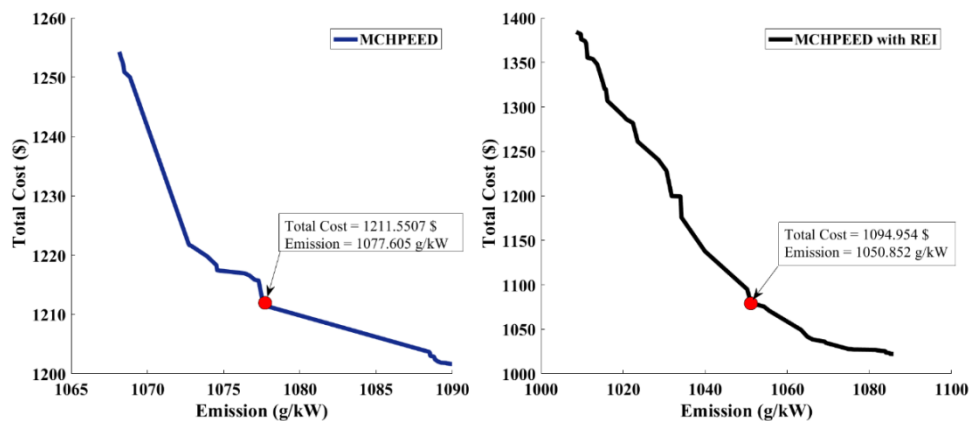


Figure 9. Pareto optimal fronts for MCHPEED and MCHPEED with REI.

For the MCHPEED problem, the BCS with the highest rank of 0.7602 (Table 8) in terms of cost and emission was found to be USD 1211.5507 and 1077.6050 g/KW, respectively.

In the case of MCHPEED with REI, total cost refers to the sum of operational costs due to fossil fuel and renewable energy resources or both. Here, the total cost of USD 1094.9539 and the emission of 1050.8518 g/kW achieved the highest topsis rank of 0.7741, considered as BCS, as shown in Table 8. Here, it was observed that the operational cost was reduced by USD 113.5980 (9.4%), and the emitted emission was reduced by 26.7532 g/kW (2.5%) due to REI. The comparison of Pareto fronts is shown in Figure 8.

4.2.4. Heat Output

As shown in Table 9, considering the hourly load demand and corresponding heat output, it was observed that heat outputs were sensitive to changes in load demand. For the MCHPEED problem, heat output was seen to be increasing and fulfilled by energy resources with an increase in load demand.

Table 9. Optimal generation scheduling for MCHPEED under BCS.

Hr.	P_1 (Dg)	P_2 (Dg)	P_3 (MT)	P_4 (Dg)	P_5 (MT)	Load (kW)	Heat (kW)
1	0.1742	43.8226	18.95	28.9484	13.7722	105	107.6286
2	0.0439	100.2222	20.8996	57.2967	15.1846	190	181.4153
3	7.9917	106.5203	41.9026	82.8549	15.4974	250	257.7412
4	34.6496	86.6041	79.7197	95.8914	16.1365	310	375.0671
5	79.0714	122.3964	76.6417	98.9171	25.9711	400	532.2534
6	111.5772	186.8943	79.5952	91.3479	24.9627	490	666.1347
7	146.7594	199.9927	78.8478	99.8593	29.8921	550	780.8991
8	256.9116	199.6686	77.2061	99.9982	29.1331	650	1061.2783
9	300.363	199.9386	79.9998	99.7264	28.9461	690	1177.0124
10	364.7395	199.1256	78.1749	99.9798	28.6631	740	1339.5097
11	377.7434	200	79.9864	98.3194	27.7766	750	1373.6715
12	353.816	197.5439	79.9687	100	27.3565	730	1310.6095
13	292.299	196.903	78.4594	99.9998	30	680	1153.3381
14	232.1257	199.7308	80	99.892	28.6524	630	1000.5748
15	183.5236	198.0663	78.5526	97.0593	29.4762	580	870.8251
16	173.3918	175.3966	64.5036	99.9331	27.4251	535	805.1119
17	137.2064	147.8064	78.3677	79.0651	21.3752	460	682.8948
18	99.7382	139.1221	67.8092	85.6515	20.4403	410	567.8843
19	59.8613	75.3932	79.433	89.8884	17.4494	320	427.6205
20	1.3002	129.0986	56.3055	76.8063	11.8101	270	269.2425
21	6.216	92.0592	22.5511	77.3491	11.2522	205	202.8413
22	2.9803	72.9563	33.5925	52.3411	10.0549	170	172.7066
23	0	58.0973	31.3545	53.8645	8.5012	150	148.3782
24	4.6627	41.2238	27.9014	23.5275	12.9832	110	124.272

However, considering Table 10 of MCHPEED with REI, it was observed that heat outputs remained increasing with load demand but were found to be lower as compared to MCHPEED. It may be due to sharing the particular range of load demand by renewable energy resources such as fuel cells and wind turbines.

Table 10. Optimal generation scheduling for MCHPEED with REI under BCS.

Hr.	$P_1(\text{Dg})$	$P_2(\text{Dg})$	$P_3(\text{FC})$	$P_4(\text{Dg})$	$P_5(\text{WPP})$	Load (kW)	Heat (kW)
1	0.4602	55.8001	0.0026	38.1092	12.2087	105	77.6358
2	0.0014	67.2099	32.6849	76.9633	16.9728	190	116.7346
3	16.6051	76.3607	49.985	97.6993	13.7738	250	183.5804
4	43.8702	95.4026	65.24	86.5622	21.4451	310	260.8134
5	2.0257	193.1514	84.1992	99.9095	31.4198	400	244.4528
6	137.9878	156.3819	94.3015	81.5604	23.9735	490	550.0218
7	172.6773	181.9743	83.4654	84.7427	33.0027	550	663.1865
8	248.3451	198.6839	88.2413	97.6099	29.5584	650	882.3438
9	339.0121	193.143	90.55	73.6115	23.326	690	1092.496
10	389.558	193.4966	93.7557	85.5281	17.9975	740	1232.578
11	372.8658	192.9266	95.0478	96.2457	27.3994	750	1197.57
12	365.0877	198.1613	72.7586	87.811	37.2745	730	1175.156
13	288.2583	183.1858	95.2879	96.5362	34.9216	680	971.5743
14	238.2183	198.1671	83.9061	83.2904	37.8205	630	844.4403
15	198.0663	199.9986	68.8349	84.5582	35.8806	580	743.4311
16	161.1864	184.6829	70.2232	89.7806	34.1974	535	639.7981
17	98.8017	154.436	88.2272	92.8929	28.9415	460	456.3623
18	33.2158	174.0753	76.4767	99.9994	33.2225	410	309.1514
19	16.428	103.6468	67.9597	97.0659	39.9701	320	205.216
20	15.2292	136.6882	29.9529	62.3144	30.3556	270	201.9077
21	0	59.1014	39.9741	90.1443	20.5677	205	120.4767
22	9.5316	78.936	2.6982	64.9587	17.4007	170	141.4918
23	1.3006	47.4008	42.5158	51.3921	8.6482	150	83.3885
24	0.2675	60.3013	12.1609	36.1635	2.3829	110	79.3222

5. Conclusions

In this paper, HHO successfully implements the planning of an MG to determine the optimal size and location of DGs and solve SCHPEED and MCHPEED problems to fulfill the particular load demand and a corresponding range of heat demand by different energy resources. The impact of REI is also investigated in both cases. Fuel cell and stochastic wind power are considered for analysis. TOPSIS is considered as a tool to obtain BCS based on the highest satisfaction level among the conflicting objectives. While comparing simulation results for the SCHPEED problem, the results obtained by HHO are found to be better compared to PSO and DE for minimum cost, minimum emission, and BCS for the multiobjective problem. The key findings are summarized below:

- HHO is simple to implement and found to be impactful for the solution of both SCHPEED and MCHPEED complex constrained optimization problems.
- With REI, fuel cost is reduced by 6.53 USD/h (18%) and emission is reduced by 1.519 g/kWh(3.4%) for SCHPEED, whereas fuel cost is reduced by USD 179.759 (14.95%) and emission is reduced by 59.60 g/kW (5.58%) for MCHPEED.
- Heat output is found to be sensitive to changes in load demand
- Operational cost, emission, and heat output are minimized with REI.

Author Contributions: Conceptualization, V.T. and H.M.D.; methodology, M.P.; software, S.R.S.; validation, V.T., H.M.D., and M.P.; formal analysis, S.R.S.; investigation, V.T.; resources, H.M.D.; data

curation, M.P.; writing—original draft preparation, V.T. and H.M.D.; writing—review and editing, H.M.D., M.P., and S.R.S.; visualization, V.T.; supervision, M.P. and S.R.S.; project administration, V.T. and H.M.D.; funding acquisition, M.P. and S.R.S. All authors have read and agreed to the published version of the manuscript.

Funding: WOOSONG UNIVERSITY’s Academic Research Funding—2022.

Institutional Review Board Statement: Not applicable.

Informed Consent Statement: Not applicable.

Data Availability Statement: Not applicable.

Acknowledgments: The authors acknowledge the support provided by WOOSONG UNIVERSITY’s Academic Research Funding—2022.

Conflicts of Interest: The authors declare no conflict of interest.

Nomenclature

FC	Fuel cell	RDS	Radial distribution system
DG	distributed generators	CHP	Combined heat and power
MG	microgrid	EED	Economic emission dispatch
WPP	Wind power plant	SCHPEED	CHP under EED for static (fixed) load
MT	Micro Turbine	MCHPEED	CHP under EED for Multiple (dynamic) load
REI	Renewable Energy Integration	BCS	Best compromise solution
k_p	penalty cost due to underestimation of wind	<i>pdf</i>	Probability distribution function
k_r	reserve cost due to overestimation of wind	V_{min}, V_{max}	Minimum and maximum voltage
k	shape factor	$F_{DG}^T, F_{WPP}^T, F_{FC}^T$	cost of thermal units, wind power plant, and fuel cell, respectively
c	scale factor	v_{cin}, v_{co}, v_r	Cut-in velocity, cut-out velocity, and rated velocity in m/s, respectively
H_R	Total heat output	θ_i	Heat-to-power ratio of i^{th} DG unit
H_D	Total heat demand.	f_1, f_2	Cost and emission function
Pfn	Price penalty factor	w	Weighting factor

References

- Alam, M.S.; Arefifar, S.A. Energy Management in Power Distribution Systems: Review, Classification, Limitations and Challenges. *IEEE Access* **2019**, *7*, 92979–93001. [\[CrossRef\]](#)
- Alipour, M.; Mohammadi-Ivatloo, B.; Zare, K. Stochastic scheduling of renewable and CHP-based microgrids. *IEEE Trans. Ind. Infor.* **2015**, *11*, 1049–1058. [\[CrossRef\]](#)
- Haghray, A.; Nazari-Heris, M.; Mohammadi-ivatloo, B. Solving combined heat and power economic dispatch problem using real coded genetic algorithm with improved mühlenbein mutation. *Appl. Therm. Eng.* **2016**, *99*, 465–475. [\[CrossRef\]](#)
- Hagh, M.T.; Teimourzadeh, S.; Alipour, M.; Aliasghary, P. Improved group search optimization method for solving CHPED in large scale power systems. *Energy Convers Manag.* **2014**, *80*, 446–456. [\[CrossRef\]](#)
- Roy, P.K.; Paul, C.; Sultana, S. Oppositional teaching learning based optimization approach for combined heat and power dispatch. *Int. J. Electr. Power Energy Syst.* **2014**, *57*, 392–403. [\[CrossRef\]](#)
- Basu, M. Modified Particle Swarm Optimization for Non-smooth Non-convex Combined Heat and Power Economic Dispatch. *Electr. Power Compon. Syst.* **2015**, *43*, 2146–2155. [\[CrossRef\]](#)
- Lashkar Ara, A.; Mohammad Shahi, N.; Nasir, M. CHP Economic Dispatch Considering Prohibited Zones to Sustainable Energy Using Self-Regulating Particle Swarm Optimization Algorithm. *Iran. J. Sci. Technol.—Trans. Electr. Eng.* **2020**, *44*, 1147–1164. [\[CrossRef\]](#)
- Nguyen, T.T.; Vo, D.N.; Dinh, B.H. Cuckoo search algorithm for combined heat and power economic dispatch. *Inter. J Electr. Power Energy Syst.* **2016**, *81*, 204–214. [\[CrossRef\]](#)
- Beigvand, S.D.; Abdi, H.; La Scala, M. Combined heat and power economic dispatch problem using gravitational search algorithm. *Electr. Power Syst. Res.* **2016**, *133*, 160–172. [\[CrossRef\]](#)
- Ghorbani, N. Combined heat and power economic dispatch using exchange market algorithm. *Inter. J. Electr. Power Energy Syst.* **2016**, *82*, 58–66. [\[CrossRef\]](#)
- Basu, M. Group search optimization for combined heat and power economic dispatch. *Inter. J. Electr. Power Energy Syst.* **2016**, *78*, 138–147. [\[CrossRef\]](#)
- Jayakumar, N.; Subramanian, S.; Ganesan, S.; Elanchezian, E.B. Grey wolf optimization for combined heat and power dispatch with cogeneration systems. *Inter. J. Electr. Power Energy Syst.* **2016**, *74*, 252–264. [\[CrossRef\]](#)

13. Dashtdar, M.; Flah, A.; Hosseinimoghadam, S.M.; Kotb, H.; Jasińska, E.; Gono, R.; Leonowicz, Z.; Jasiński, M. Optimal Operation of Microgrids with Demand-Side Management Based on a Combination of Genetic Algorithm and Artificial Bee Colony. *Sustainability* **2022**, *14*, 6759. [[CrossRef](#)]
14. Chiñas-Palacios, C.; Vargas-Salgado, C.; Aguila-Leon, J.; Hurtado-Pérez, E. A Cascade Hybrid PSO Feed-Forward Neural Network Model of a Biomass Gasification Plant for Covering the Energy Demand in an AC Microgrid. *Energy Convers. Manag.* **2021**, *232*, 113896. [[CrossRef](#)]
15. Aguila-Leon, J.; Chiñas-Palacios, C.; Garcia, E.X.M.; Vargas-Salgado, C. A Multimicrogrid Energy Management Model Implementing an Evolutionary Game-Theoretic Approach. *Int. Trans. Electr. Energy Syst.* **2020**, *30*, e12617. [[CrossRef](#)]
16. Barbosa-Ayala, O.I.; Montañez-Barrera, J.A.; Damian-Ascencio, C.E.; Saldaña-Robles, A.; Alfaro-Ayala, J.A.; Padilla-Medina, J.A.; Cano-Andrade, S. Solution to the Economic Emission Dispatch Problem Using Numerical Polynomial Homotopy Continuation. *Energies* **2020**, *13*, 4281. [[CrossRef](#)]
17. Ahmadi, A.; Moghimi, H.; Nezhad, A.E.; Agelidis, V.G.; Sharaf, A.M. Multiobjective economic emission dispatch considering combined heat and power by normal boundary intersection method. *Electr. Power Syst. Res.* **2015**, *129*, 32–43. [[CrossRef](#)]
18. Shaabani, Y.A.; Seifi, A.R.; Kouhanjani, M.J. Stochastic multiobjective optimization of combined heat and power economic/emission dispatch. *Energy* **2017**, *141*, 1892–1904. [[CrossRef](#)]
19. Jayakumar, N.; Subramanian, S.; Ganesan, S.; Elanchezian, E.B. Combined heat and power dispatch by grey wolf optimization. *Inter. J. Energy Sect. Manag.* **2015**. [[CrossRef](#)]
20. Sundaram, A. Multiobjective multi-verse optimization algorithm to solve combined economic, heat and power emission dispatch problems. *Appl. Soft Comp.* **2020**, *91*, 106195. [[CrossRef](#)]
21. Dubey, H.M.; Pandit, M.; Panigrahi, B.K. An overview and comparative analysis of recent bio-inspired optimization techniques for wind integrated multiobjective power dispatch. *Swarm Evol. Comp.* **2018**, *38*, 12–34. [[CrossRef](#)]
22. Basu, M.; Chowdhury, A. Cuckoo search algorithm for economic dispatch. *Energy* **2013**, *60*, 99–108. [[CrossRef](#)]
23. Basu, M. Squirrel Search Algorithm for Multi-region Combined Heat and Power Economic Dispatch Incorporating Renewable Energy Sources. *Energy* **2019**, *182*, 296–305. [[CrossRef](#)]
24. Dubey, S.M.; Dubey, H.M.; Pandit, M.; Salkuti, S.R. Multiobjective Scheduling of Hybrid Renewable Energy System Using Equilibrium Optimization. *Energies* **2021**, *14*, 6376. [[CrossRef](#)]
25. Jin, J.; Wen, Q.; Zhang, X.; Cheng, S.; Guo, X. Economic Emission Dispatch for Wind Power Integrated System with Carbon Trading Mechanism. *Energies* **2021**, *14*, 1870. [[CrossRef](#)]
26. Vargas-Salgado, C.; Berna-Escriche, C.; Escrivá-Castells, A.; Díaz-Bello, D. Optimization of All-Renewable Generation Mix According to Different Demand Response Scenarios to Cover All the Electricity Demand Forecast by 2040: The Case of the Grand Canary Island. *Sustainability* **2022**, *14*, 1738. [[CrossRef](#)]
27. Tiwari, V.; Dubey, H.M.; Pandit, M. Economic Dispatch in Renewable Energy Based Microgrid Using Manta Ray Foraging Optimization. In Proceedings of the 2nd International Conference on Electrical Power and Energy Systems (ICEPES 2021), Online Mode, 10–11 December 2021; pp. 1–6. [[CrossRef](#)]
28. Harsh, P.; Das, D. Energy Management in Microgrid Using Incentive-Based Demand Response and Reconfigured Network Considering Uncertainties in Renewable Energy Sources. *Sustain. Energy Technol. Assess.* **2021**, *46*, 101225. [[CrossRef](#)]
29. Anand, H.; Narang, N.; Dhillon, J.S. Multi-Objective Combined Heat and Power Unit Commitment Using Particle Swarm Optimization. *Energy* **2019**, *172*, 794–807. [[CrossRef](#)]
30. Rezaee Jordehi, A. A Mixed Binary-continuous Particle Swarm Optimisation Algorithm for Unit Commitment in Microgrids Considering Uncertainties and Emissions. *Int. Trans. Electr. Energy Syst.* **2020**, *30*, e12581. [[CrossRef](#)]
31. Hetzer, J.; Yu, D.C.; Bhattarai, K. An economic dispatch model incorporating wind power. *IEEE Trans. Energy Convers* **2008**, *23*, 603–611. [[CrossRef](#)]
32. Basu, A.K.; Bhattacharya, A.; Chowdhury, S.; Chowdhury, S.P. Planned scheduling for economic power sharing in a CHP-based micro-grid. *IEEE Tran. Power Syst.* **2011**, *27*, 30–38. [[CrossRef](#)]
33. Wolpert, D.H.; Macready, W.G. No free lunch theorems for optimization. *IEEE Trans. Evol. Comp.* **1997**, *1*, 67–82. [[CrossRef](#)]
34. Heidari, A.A.; Mirjalili, S.; Faris, H.; Aljarah, I.; Mafarja, M.; Chen, H. Harris hawks optimization: Algorithm and applications. *Future Gener. Comput. Syst.* **2019**, *97*, 849–872. [[CrossRef](#)]
35. Abdelsalam, M.; Diab, H.Y.; El-Bary, A.A. A Metaheuristic Harris Hawk Optimization Approach for Coordinated Control of Energy Management in Distributed Generation Based Microgrids. *Appl. Sci.* **2021**, *11*, 4085. [[CrossRef](#)]
36. Hong, L.; Rizwan, M.; Rasool, S.; Gu, Y. Optimal Relay Coordination with Hybrid Time–Current–Voltage Characteristics for an Active Distribution Network Using Alpha Harris Hawks Optimization. *Eng. Proc.* **2021**, *12*, 26. [[CrossRef](#)]
37. Hwang, C.L.; Yoon, K.P. *Multiple Attribute Decision Making: Methods and Applications*; Springer: New York, NY, USA, 1981. [[CrossRef](#)]